International Science and Technology Journal
المجلة الدولية للعلوم والتقنية
Volume 33 العدد
Part 2 المجلد
January 2024 يناير
المجلة الدولية للعلوم والتقنية
ISTJ
تم استلام الورقة بتاريخ: 2023/12/29م وتم نشرها على الموقع بتاريخ: 29/ 1/2024م

A finite element analysis (FEA) of the vibration characteristics of a subsea gas pipeline

Mohammed Eliwa
Faculty of engineering- Azzaytuna University,
Email: Zalaff78@gmail.com

Abstract:
The main objective of this research is to use finite element analysis (FEA) of vibration characteristics of a subsea gas pipeline using MATLAB. The purpose is to study the pipeline's natural frequencies and mode shapes. In addition, these calculations will help examine the natural frequency values to determine the suitability of the pipeline to operate within the ocean current. These values later converged to the conditions stipulated in the DNV-RP-105F Directive (Free Extension Pipelines, 2006), where it was discovered whether VIV (vortex-induced vibration) was generated with cross-flow.

Keywords: gas pipeline, vibrations, FEA, frequencies and MATLAB

تحليل العناصر المحدودة (FEA) لخصائص الاهتزاز لخط أنابيب الغاز تحت سطح البحر

محمد عليوه محمد عليوه
كلية الهندسة – جامعة الزيتونة
Email: Zalaff78@gmail.com

الملخص:
الهدف الرئيسي من هذا البحث هو استخدام تحليل العناصر المحدودة (FEA) لخصائص الاهتزاز لخط أنابيب الغاز تحت سطح البحر باستخدام MATLAB. والغرض من ذلك هو دراسة الترددات الطبيعية لخط الأنابيب وأشكال الأوضاع. بالإضافة إلى أن هذه الحسابات سوف تساعد على فحص قيم التردد الطبيعي لتحديد مدى ملاءمة خط الأنابيب للعمل ضمن التيار المحيطي. تقاربت هذه القيم لاحقًا مع الشروط المنصوص عليها في

تم استلام الورقة بتاريخ: 2023/12/29م وتم نشرها على الموقع بتاريخ: 29/ 1/2024م

توجيه DNV–RP–105F (خطوط الأنابيب الممتدة المجانية، 2006)، حيث تم اكتشاف ما إذا كان VIV (الاهتزاز الناجم عن الدوامة) قد تم إنشاؤه باستخدام التدفق المتقاطع.
الكلمات المفتاحية: أنابيب الغاز ,الاهتزازات ,تحليل العناصر المحدودة ,الترددات و المتلاب.

1. Introduction:

Undersea gas transportation pipelines have become one of the most important tools to help transfer energy to the consumer in the fastest time and at the lowest cost. However, the complexity of subsea systems is rising as they are built and used at ever-deeper water levels. One factor that is frequently disregarded is the risk posed by vibration, which can result in serious problems with integrity and dependability. The subsea pipeline is an integral infrastructure component used throughout industry such as in oil and gas networks. Laying pipes along the seabed requires sound engineering because of issues, which may arise; bending stresses, buckling, and vibrations are the most common. This report will examine vertical transverse natural frequencies for a free-span pipeline over a sleeper. A sleeper initiates buckling and is commonly used in the oil and gas industry [1]. The FEA used in this report indicates that the pipeline is suitable. The correlation established between analytical and pipeline model results indicate that the simple pipeline model sufficiently describes the pipeline system. An analysis of the recommended practice and the results generated indicates that subsequent VIV modelling may help boost the quality of the results. The convergence of the lumped and consistent mass matrices fuels more confidence in the model developed.

2. The design and the parameters of the Pipeline Model

As shown in table (1) below, some assumptions of physical properties of steel pipeline such as the Young's Modulus and density values with seabed material of sand.

تم استلام الورقة بتاريخ: 2023/12/29م وتم نشرها على الموقع بتاريخ: 29/ 1/2024م

Table 1 Parameters of the Pipeline Model

Parameter	Value
Young's modulus for steel(E)	$200\times 10^9 Pa$
Span Length from sleeper to seabed (L)	$39\ m$
Pipe Cross Sectional Area (A)	$0.0519 m^2$
Density of Pipe Material (ρ)	$7850\ kg/m^3$
Moment of inertia for steel(I)	$0.00146\ m^4$
Nominal Mean current speed(v)	1.5 m/s
Pipe Diameter (D)	$508\ mm$
Sleeper Height (H)	$2\ m$
Pipe Thickness (t)	$34.9\ mm$

2.1 The profile shapes:

An investigation of profile shapes reveals how they affect the natural frequencies. They are as follows:

Catenary:

Its curve is formed when gravity acts on a chain or rope and it may result in as:

$$y = a\cosh\left(\frac{x}{a}\right) + b \quad (1)$$

Linear:

This is the simplest profile and boasts a constant slope. The correlation between distance and height may be expressed in the form outlined below.

$$y = ax + b \quad (2)$$

Logistic:

This is predominantly used for statistics and has an extra feature the other curves do not possess: the function tends towards $\pm\infty$ and the curve tends towards two different heights [2]. This may be written in the form outlined below:

$$y = \frac{a}{1 + e^{-b(x-c)}} \quad (3)$$

Parabolic:

Correlation of the parabolic shape between both of the height and distance which can be apply on Euler-Bernoulli beams utilise this correlation and it is written in the following form:

$$y = ax^2 + bx + c \quad (4)$$

تم استلام الورقة بتاريخ: 2023/12/29م وتم نشرها على الموقع بتاريخ: 29/ 1/2024م

2.2 Theoritical flexural vibration of fuler-bernoouli beams:

In order to analyse the beam's characteristics during transverse flexure, the Euler-Bernoulli beam model has been used [3]. The beam's motion is derived with the bending effects and therefore the genearl differential equation for the Euler-Bernoulli beam is as follows:

$$EI\frac{d^4w}{dx^4} = q(x) \qquad (5)$$

To calculate the equation of natural frequency for any beam can be determine by using the Euler-Bernoulli beam model with two degrees, such as slope and deflection as expressed below:

$$\omega r = \lambda_{r^2}\sqrt{\frac{EI}{A\rho}} \qquad (6)$$

The λ_r is presented the beam's end conditions and the vibration mode. As displayed below, the end conditions need to satisfy the pipeline's characteristics.

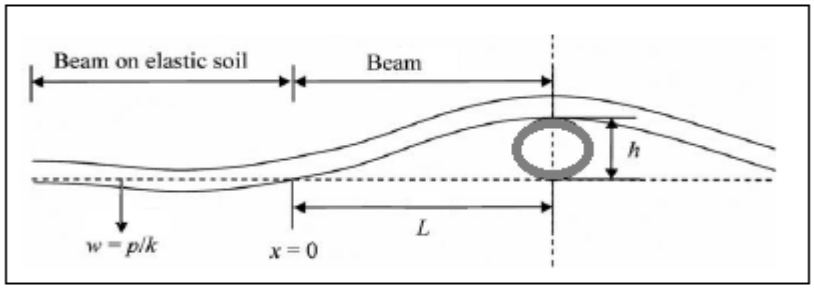

Figure 1. The characteristics of the pipeline model

The postion of the pipe line as shown above in figuer (1) which is steay on the seabed with possible movments or even rotaions because of its setting on top of the sleeper, so the ends conditons of the pipe line could be pinned, clamped,Spring-Pinned,Pinned-Pinned or even Clamped-Pinned . As a result of the seabed stiffness, the seabed will be as a spring.

تم استلام الورقة بتاريخ: 2023/12/29م وتم نشرها على الموقع بتاريخ: 29/ 1/2024م

2.3 Finite Element Analysis of Subsea Pipeline:

By assuming the the axial forces on the pipeline are negligible and it is free of external forces except for VIV. Morover, this model also neglects the effects of temperature change along the pipeline during operation. The Euler-Bernoulli beam element can be modelled in a finite element form as shown below including [4] .

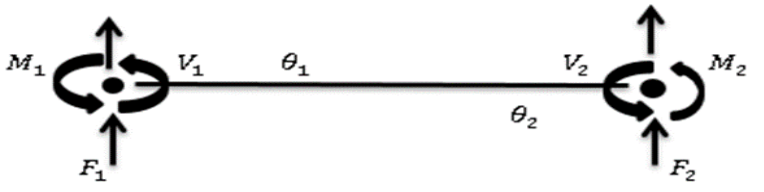

(a)

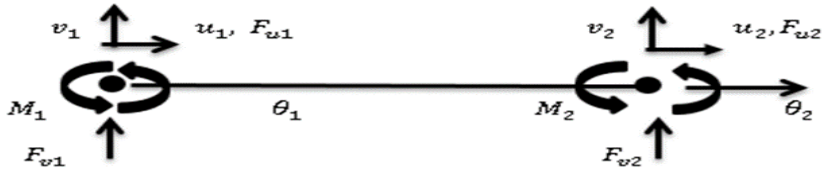

(b)

Figure 1. (a), The model with without Axial Effects
(b). The model under the effects of axial deflection

The mass of every element can be dispersed into different methods as displayed below:
Consistent Mass Element is:

$$M_e = \frac{\rho AL}{420}\begin{bmatrix} 140 & 0 & 0 & 70 & 0 & 0 \\ 0 & 156 & 22L & 0 & 54 & -13L \\ 0 & 22L & 4L^2 & 0 & 13L & -3L^2 \\ 70 & 0 & 0 & 140 & 0 & 0 \\ 0 & 54 & 13L & 0 & 156 & -22L \\ 0 & -13L & -3L & 0 & -22L & 4L^2 \end{bmatrix}\begin{bmatrix} u_1 \\ v_1 \\ \theta_1 \\ u_2 \\ v_2 \\ \theta_2 \end{bmatrix}$$

Where the Lumped Mass Element is:

International Science and Technology Journal
المجلة الدولية للعلوم والتقنية
Volume 33 العدد
Part 2 المجلد
January 2024 يناير
المجلة الدولية للعلوم والتقنية
ISTJ
تم استلام الورقة بتاريخ: 2023/12/29م وتم نشرها على الموقع بتاريخ: 29/ 1/2024م

$$M_e = \frac{\rho AL}{2}\begin{bmatrix} 1 & 0 & 0 & 0 & 0 & 0 \\ 0 & 1 & 0 & 0 & 0 & 0 \\ 0 & 0 & \frac{L^2}{12} & 0 & 0 & 0 \\ 0 & 0 & 0 & 1 & 0 & 0 \\ 0 & 0 & 0 & 0 & 1 & 0 \\ 0 & 0 & 0 & 0 & 0 & \frac{L^2}{12} \end{bmatrix}\begin{bmatrix} u_1 \\ v_1 \\ \theta_1 \\ u_2 \\ v_2 \\ \theta_2 \end{bmatrix}$$

Fortheremoe, The stiffness for the elements can be classified by the subsequent,

Stiffness Element of the pipeline system:

$$\begin{bmatrix} \frac{AL^2}{I} & 0 & 0 & -\frac{AL^2}{I} & 0 & 0 \\ 0 & 12 & 6L & 0 & -12 & 6L \\ 0 & 6L & 4L^2 & 0 & -6L & 2L^2 \\ \frac{-AL^2}{2} & 0 & 0 & \frac{AL^2}{I} & 0 & 0 \\ 0 & -12 & -6L & 0 & 12 & -6L \\ 0 & 6L^2 & 2L^2 & 0 & -6L & 4L^2 \end{bmatrix}\begin{matrix} u_1 \\ v_1 \\ \theta_1 \\ u_2 \\ v_2 \\ \theta_2 \end{matrix}$$

The spring constriction can be modelled as below,

تم استلام الورقة بتاريخ: 2023/12/29م وتم نشرها على الموقع بتاريخ: 29/ 1/2024م

$$K_e = \frac{EI}{L^1}\begin{bmatrix} \frac{AL^2}{I} & 0 & 0 & -\frac{AL^2}{I} & 0 & 0 \\ 0 & 12+\frac{L^3 k_{spring}}{EI} & 6L & 0 & -12 & 6L \\ 0 & 6L & 4L^2 & 0 & -6L & 2L^2 \\ -\frac{AL^2}{I} & 0 & 0 & \frac{AL^2}{I} & 0 & 0 \\ 0 & -12 & -6L & 0 & 12 & -6L \\ 0 & 6L & 2L^2 & 0 & -6L & 4L^2 \end{bmatrix}\begin{bmatrix} u_1 \\ v_1 \\ \theta_1 \\ u_2 \\ v_2 \\ \theta_2 \end{bmatrix}$$

To enable the rotation of stiffness and mass elements, The transformation matrix can be apply as below,
The Transformation Matrix would be:

$$\boldsymbol{T} = \begin{bmatrix} \cos\theta & \sin\theta & 0 & 0 & 0 & 0 \\ -\sin\theta & \cos\theta & 0 & 0 & 0 & 0 \\ 0 & 0 & 1 & 0 & 0 & 0 \\ 0 & 0 & 0 & \cos\theta & \sin\theta & 0 \\ 0 & 0 & 0 & -\sin\theta & \cos\theta & 0 \\ 0 & 0 & 0 & 0 & 0 & 1 \end{bmatrix}\begin{bmatrix} u_1 \\ v_1 \\ \theta_1 \\ u_2 \\ v_2 \\ \theta_2 \end{bmatrix}$$

The both of the stiffness and mass matrices can be transformed by thefollowing equations respectivilly,

$$k = \mathrm{T}' k_e \, T \qquad (7)$$

$$M = \mathrm{T}' M_e \, T \qquad (8)$$

With consider that the slope (θ) for the all shapes can be estimated by the average gradient function as presented below.

$$\theta = tan^{-1}\left[\frac{y_2 - y_2}{x_2 - x_1}\right] \qquad (9)$$

The figure (2) below shows the idea of brokenthe pipeline into number of the elements.

International Science and Technology Journal
المجلة الدولية للعلوم والتقنية
Volume 33 العدد
Part 2 المجلد
January 2024 يناير
المجلة الدولية للعلوم والتقنية
ISTJ
تم استلام الورقة بتاريخ: 2023/12/29م وتم نشرها على الموقع بتاريخ: 29/ 1/2024م

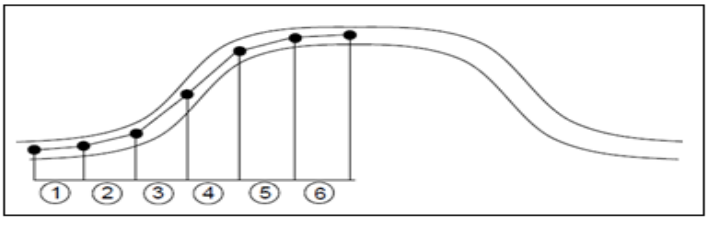

Figure 2. The pipeline elements

2.4 stiffniss modelling of the seabed:

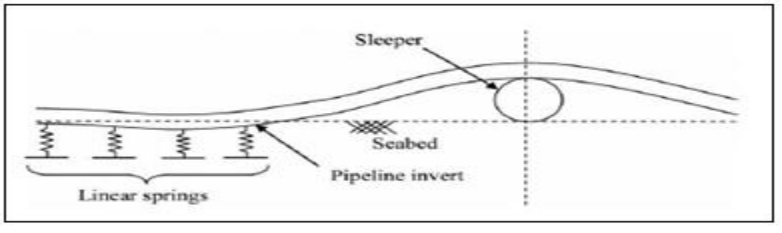

Figure 3. The modelling of the seabed.

The stiffniss for a model[5] shown in figure 3 and with using the static stiffness values for pipe-soil interaction in sand from the data which have given in table 2 below,

Table 2. Dynamic stiffness factor and static stiffness for pipe-interaction in sand

Sand type	$C_V\ (\frac{kN}{m^2})$	$C_L\ (\frac{kN}{m^2})$	$C_{V,S}\ (\frac{kN}{m^2})$
Loose	10500	9000	250
Medium	14500	12500	530
Dense	21000	18000	1350

The spans lenght between the sleepers in usually are between 2 to 3 kilometres. The spring stiffness of the system with a single spring at one end can be calculated by the following equations[6]. Where is the length presented the length of the pipe in contact with the seabed.

$$k_{spring} = \frac{k_{v,s} \times L}{2} \qquad (10)$$

$$Lmin = 2000 - (2 \times 39) = 1922\ m$$

تم استلام الورقة بتاريخ: 2023/12/29م وتم نشرها على الموقع بتاريخ: 29/ 1/2024م

$$Lmax = 3000 - (2 \times 39) = 2922m$$

Likewise, the minimum spring stiffness of the sand if loose can be,

$$k_{spring(min)} = \frac{250{,}000 \times 1922}{2} = 2.4 \times 10^8 N/m$$

The maximum spring stiffness of the sand in case of dense can be,

$$k_{spring(min)} = \frac{1{,}350{,}000 \times 2922}{2} = 1.972 \times 10^9 N/m$$

In addition, the sleeper lengths range between 25 to 50 metres. The corresponding spring stiffness, as it rests on the sleeper, may be simplified to a linear spring. The sleeper directly transfers the pipeline forces to the seabed. So, the minimum spring stiffness would be,

$$k_{sleeper(min)} = 250{,}000 \times 25 = 6.25 \times 10^6 N/m$$

The maximum spring stiffness,

$$k_{sleeper(max)} = 1{,}350{,}000 \times 50 = 6.75 \times 10^7 N/m$$

3. Analysis of the FEM without Axial Effects:

3.1 Examination of the different profile shapes under the different end condition with using consistent mass matrix.

The Results shown in Table 3 indicate that natural frequencies for each end condition remain very close irrespective of the profile shape. The standard deviations range from 0.00115 to 0.00118 Hz. It is clear by neglecting the effects of axial movement means that the particular shape of the pipeline bears little influence on the natural frequencies. The natural frequencies are also very similar for both the pinned-pinned and spring-pinned end conditions [7]. It should also be mentioned that according to DNV-RP-105F the natural frequency of most interest is the lowest and therefore the pinned-pinned end condition is selected.

تم استلام الورقة بتاريخ: 2023/12/29م وتم نشرها على الموقع بتاريخ: 29/ 1/2024م

Table 3. The frequencies of different profile shapes under the different end condition

Profile Shape	Natural Frequency	Clamped-Pinned	Pinned-Pinned	Spring-Pinned $k_{sleeper(min)} = 2.4 \times 10^8 \mathrm{N/m}$	Spring-Pinned $k_{sleeper(min)} = 1.972 \times 10^9 N/m$
Logistic	$\omega_1(HZ)$	1.29656	0.83039	0.83023	0.83037
	$\omega_2(HZ)$	4.18317	3.30135	3.29889	3.30105
Parabolic	$\omega_1(HZ)$	1.29407	0.82798	0.82782	0.82796
	$\omega_2(HZ)$	4.19419	3.31349	3.31101	3.31319
Catenary	$\omega_1(HZ)$	1.29406	0.82797	0.82782	0.82795
	$\omega_2(HZ)$	4.19416	3.31346	3.31099	3.31316
Linear	$\omega_1(HZ)$	1.29516	0.82906	0.82890	0.82904
	$\omega_2(HZ)$	4.19780	3.31657	3.31408	3.31626
Standard Deviation	$\omega_1(HZ)$	0.00118	0.00115	0.00115	0.00115
	$\omega_2(HZ)$	0.00634	0.00674	0.00673	0.00674

3.2 Comparison with lumped mass matrix

There is a small change in the natural frequencies at every different profile forms in term of using the lumped mass matrix to calculate the natural frequencies of the pipeline see table 4 below. By analysing the flat pipeline situation with FEM, the two lowest natural frequencies of the consistent mass matrix of a pinned-pinned system are:

$$\omega_1 = 0.83113\ HZ$$
$$\omega_2 = 3.32450\ HZ$$

تم استلام الورقة بتاريخ: 2023/12/29م وتم نشرها على الموقع بتاريخ: 29/ 1/2024م

Similarly, using the lumped mass matrix, the two lowest natural frequencies would be:

$$\omega_1 = 0.83091 \ HZ$$
$$\omega_2 = 3.32109 \ HZ$$

Table 4. The frequencies of different profile shapes with using lumped mass matrix

Profile Shape	Natural Frequency	Lumped Mass Matrix Pinned-Pinned	Consistent Mass Matrix Pinned-Pinned
Logistic	$\omega_1(HZ)$	0.83019	0.83039
	$\omega_2(HZ)$	3.29699	3.30135
Parabolic	$\omega_1(HZ)$	0.82775	0.82798
	$\omega_2(HZ)$	3.30934	3.31349
Catenary	$\omega_1(HZ)$	0.82774	0.82797
	$\omega_2(HZ)$	3.30932	3.31346
Linear	$\omega_1(HZ)$	0.82883	0.82906
	$\omega_2(HZ)$	3.31243	3.31657
Standard Deviation	$\omega_1(HZ)$	0.00116	0.00115
	$\omega_2(HZ)$	0.00 684	0.00674

4. Analysis of the FEM with Axial Effects:

4.1 Examination of the different profile shapes under the different end conditions by using consistent mass matrix

Table 5 presents the results, which indicate that there is a significant variation in the natural frequencies according to profile shapes. The standard deviations range between 0.38582 to 1.55807 Hz. There is minimal difference in natural frequencies across the various end conditions. This indicates that with the presence of pipeline axial movements the profile shape has a substantial impact on the natural frequencies. Moreover, the pinned-pinned and spring-pinned end conditions registered close to identical natural frequencies.

International Science and Technology Journal
المجلة الدولية للعلوم والتقنية
Volume 33 العدد
Part 2 المجلد
January 2024 يناير
المجلة الدولية للعلوم والتقنية
ISTJ
تم استلام الورقة بتاريخ: 2023/12/29م وتم نشرها على الموقع بتاريخ: 29/ 1/2024م

Table 5 the natural frequencies of the different profile shapes under the different end conditions

Profile Shape	Natural Frequency	Clamped-Pinned	Pinned-Pinned	Spring-Pinned $k_{sleeper(min)} = 2.4 \times 10^8$N/m	Spring-Pinned $k_{sleeper(min)}$ =1.972× $10^9 N/m$
Logistic	$\omega_1(HZ)$	1.43386	0.82720	0.82704	0.82718
	$\omega_2(HZ)$	6.78844	6.42911	5.13873	6.18344
Parabolic	$\omega_1(HZ)$	2.14447	1.97538	1.49547	1.87905
	$\omega_2(HZ)$	4.19579	3.31138	3.30891	3.31108
Catenary	$\omega_1(HZ)$	2.14687	1.97776	1.49700	1.88126
	$\omega_2(HZ)$	4.19567	3.31135	3.30888	3.31105
Linear	$\omega_1(HZ)$	1.29514	0.82905	0.82890	0.82903
	$\omega_2(HZ)$	4.19708	3.31621	3.31373	3.31591
Standard Deviation	$\omega_1(HZ)$	0.45455	0.66306	0.38582	0.607402
	$\omega_2(HZ)$	1.29613	1.55807	0.91412	1.435382

4.2 The Mode shapes:

Pinned-Pinned:

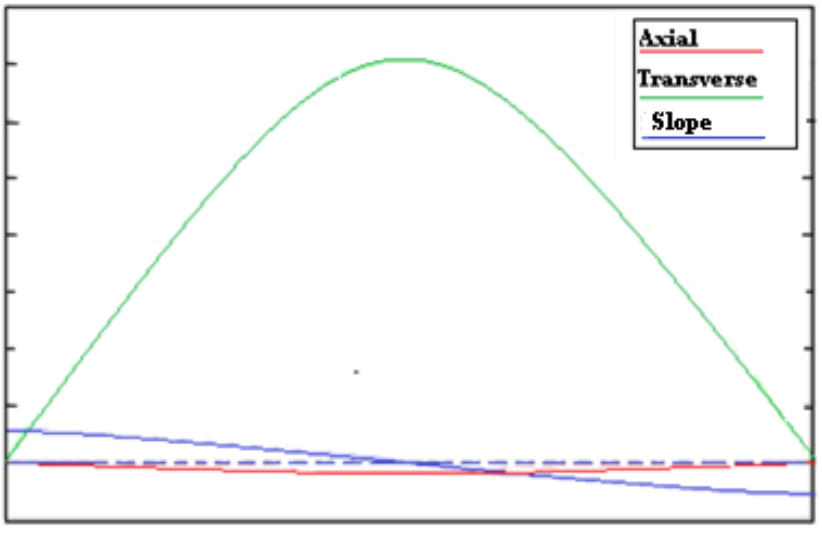

Figure 4. The First Natural Frequency

تم استلام الورقة بتاريخ: 2023/12/29م وتم نشرها على الموقع بتاريخ: 29/ 1/2024م

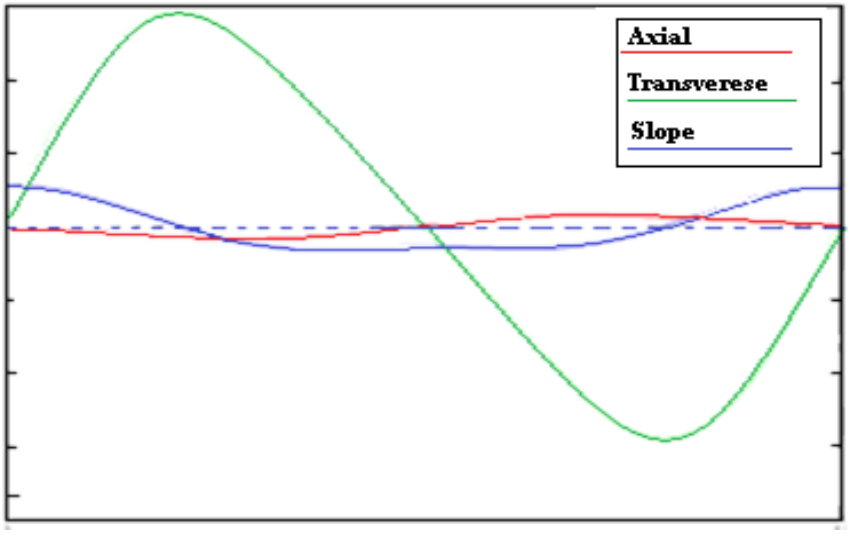

Figure 5. The Second Natural Frequency

Clamped-Pinned:

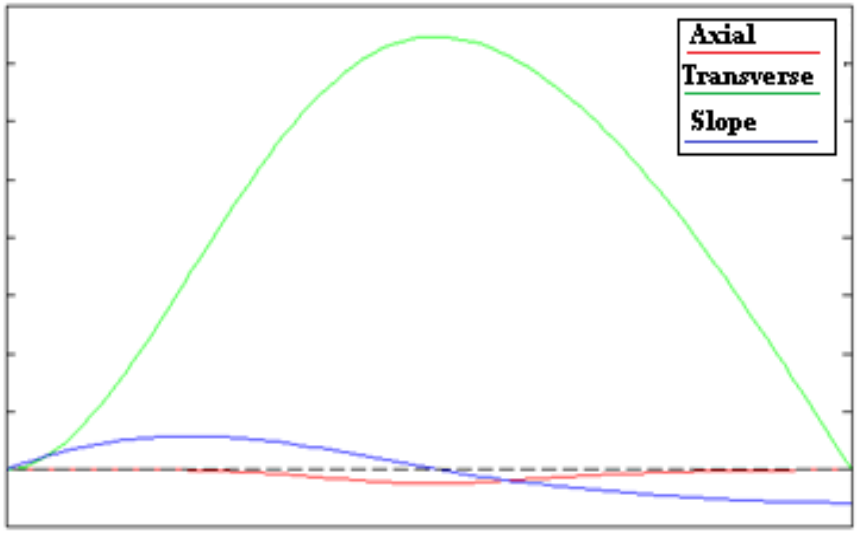

Figure 6. The First Natural Frequency

International Science and Technology Journal
المجلة الدولية للعلوم والتقنية
Volume 33 العدد
Part 2 المجلد
January 2024 يناير
المجلة الدولية للعلوم والتقنية
ISTJ
تم استلام الورقة بتاريخ: 2023/12/29م وتم نشرها على الموقع بتاريخ: 29/ 1/2024م

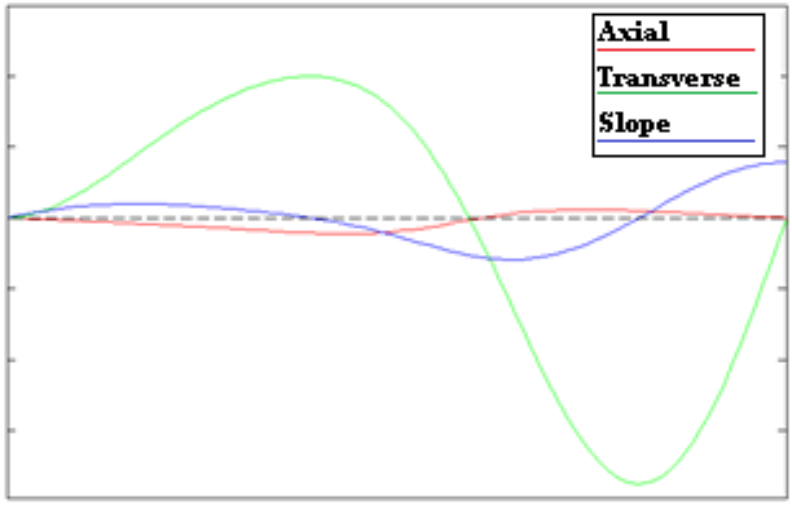

Figure 7. The Second Natural Frequency

5. Analysis of Specialised End Conditions:

5.1 The Analysis:

To fully model the Subsea Pipeline (see Figure 8 below), a more accurate representation of the Pipeline Seabed span must first be created. [8]. This may be achieved by extending the pipeline further along the seabead (level ground is assumed) using a sequence of linear beads to fix the pipeline to the ground as,

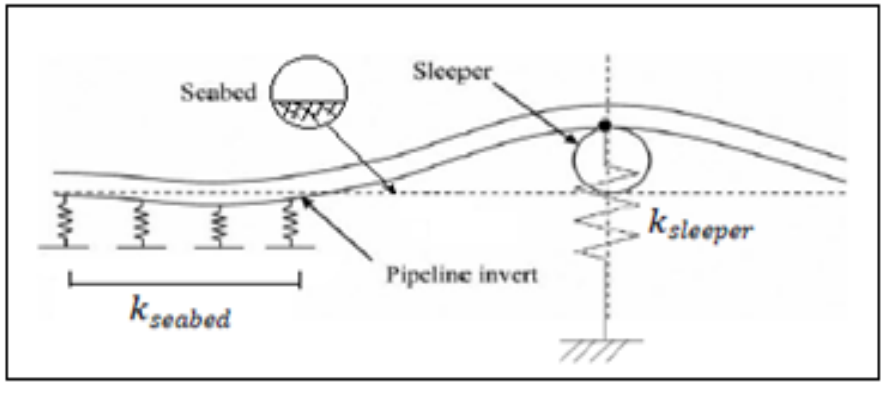

Figure8. The subsea pipeline model.

تم استلام الورقة بتاريخ: 2023/12/29م وتم نشرها على الموقع بتاريخ: 29/ 1/2024م

Thus the axial direction required to be constraining with assuming they are equal transverse direction. On the right side of the modle with these boundary conditions, would be expected the sleeper is rigid with join the pipeline to the seabed, therefore it can be work as another linear spring [9]. The seabed length was assumed in this model to be around 100 meters beyond the pipeline while contacting the seabed,as well as the length for the elements separtilly are 0.4 m. The table 6 below shows the lowest frequencies are found within the linear and logistic profiles, the seabed stiffness that corresponds with loose sand, and the sleeper that has the lowest stiffness.

Table 6. Lowest frequencies within the linear and logistic profiles

Profile Shape	Natural Frequency	$k_{seabed(min)} = 250 \times 10^3 N/m^2$		$k_{seabed(max)} = 1350 \times 10^3 N/m^2$	
		$k_{s\,(min)}$	$k_{s\,(max)}$	$k_{s\,(min)}$	$k_{s(max)}$
Logistic	$\omega_1(HZ)$	0.86103	0.86645	0.98772	0.99507
	$\omega_2(HZ)$	2.62549	2.74477	3.14707	3.68334
Parabolic	$\omega_1(HZ)$	0.89613	0.97546	1.02323	1.19378
	$\omega_2(HZ)$	2.57178	2.61075	3.08082	3.15030
Catenary	$\omega_1(HZ)$	0.89622	0.97574	1.02333	1.19432
	$\omega_2(HZ)$	2.57177	2.61073	3.08080	3.15026
Linear	$\omega_1(HZ)$	0.86379	0.87174	0.98964	0.99823
	$\omega_2(HZ)$	2.57704	2.62276	3.08575	3.16182
Standard Deviation	$\omega_1(HZ)$	0.019527	0.061529	0.019992	0.113976
	$\omega_2(HZ)$	0.026098	0.065258	0.03239	0.264663

تم استلام الورقة بتاريخ: 2023/12/29م وتم نشرها على الموقع بتاريخ: 29/ 1/2024م

5.2 Mode shape of pipe line:

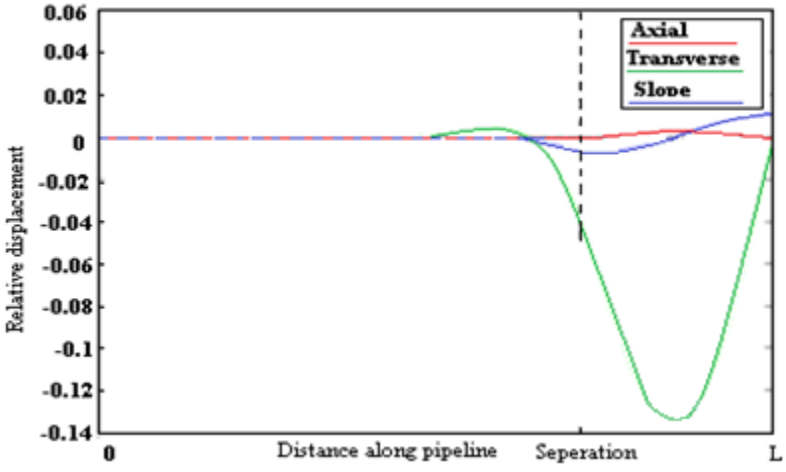

Figure 9. The lowest natural frequency's mode shapes

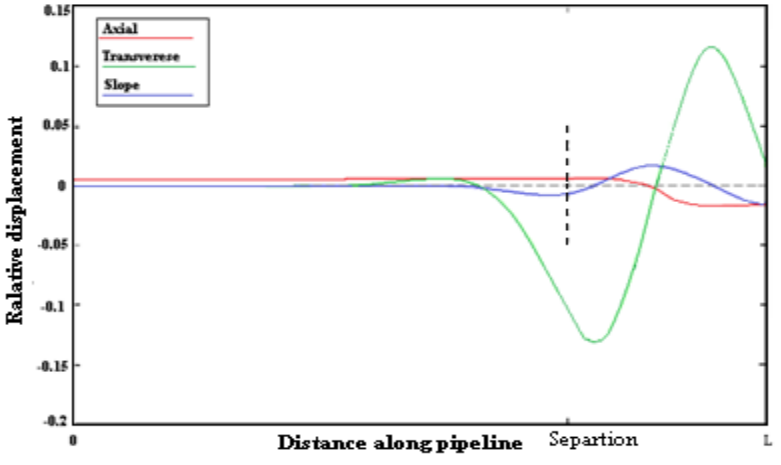

Figure 10. The second natural frequency's mode shapes

6. Conclusions:

Due to the pipe span's unsupported length, vortex-induced vibration (VIV) occurs when the ocean current flows around it. Furthermore, because the pipeline is positioned atop the sleepers, its location on the seabed may move or even rotate. As a result, the pipeline's ends

تم استلام الورقة بتاريخ: 2023/12/29م وتم نشرها على الموقع بتاريخ: 29/ 1/2024م

may be clamped, pinned, spring-pinned, pinned-pinned, or even clamp-pinned. The seafloor will behave like a spring because of its rigidity. A range of different natural frequencies and mode shapes of the pipeline system model have been analysed in this report with different end conditions, also in terms of getting more knowledge about the vibrating features of the pipeline. Moreover, using the finite element analysis (FEA) model developed helps to analyse the problem by examining the model of the Euler-Bernoulli beam and to get a high correlation with the estimated results, in this report. In addition, it has become clear that the fluid cross flow can excite the first natural frequency of the pipeline, and also by analysing a number of end conditions and different configurations, this has been analysed in contrast to the (DNV-RP-105F: Free Spanning Pipelines 2006).

7. References:

[1]Lin, Y. Z., Xue, J. H., & Tang, M. Q. (2014, January). Finite-Element Analysis of Buckle Propagation in Offshore Pipelines. Applied Mechanics and Materials, 488–489, 1039–1042.

[2]Bruton, D.A.S., M. Carr and F. Sinclair. 2011. “Geotechnical challenges for deepwater pipeline design – SAFEBUCK JIP.” Frontiers in Offshore Geotechnics II

[3]Shames, I. H., Dym, C. L., & Saunders, H. (2018). Energy and finite element methods in structural mechanics. In Routledge eBooks. https://doi.org/10.1201/9780203757574

[4]Cook, R. D., Malkus, D. S., Plesha, M. E., & Witt, R. (1974). Concepts and applications of Finite element Analysis. https://cds.cern.ch/record/1501160

[5]White, F. 1999. Fluid Mechanics. Boston, Massachusetts: McGraw-Hill.

[6]Westgate Z.J., M.F. Randolph and D.J. White. 2011. “Theoretical, numerical and field studies of offshore pipeline sleeper crossings.” Frontiers in Offshore Geotechnics II.

[7]Fofonoff, N. P. (1985). Physical properties of seawater: A new salinity scale and equation of state for seawater. Journal of

تم استلام الورقة بتاريخ: 2023/12/29م وتم نشرها على الموقع بتاريخ: 29/ 1/2024م

Geophysical Research, 90(C2), 3332–3342. https://doi.org/10.1029/jc090ic02p0333.

[8]White, D. J. (2010b). Frontiers in Offshore Geotechnics II. In CRC Press eBooks. https://doi.org/10.1201/b10132

[9]Det Norske Veritas, DNV-RP-105F, Free Spanning Pipelines, February 2006. http://exchange.dnv.com/publishing/codes/download.asp?url=2006-02/rp-f105.pdf